

Procedures for Characterizing an Alloy and Predicting Cyclic Life With the Total Strain Version of Strainrange Partitioning

James F. Saltsman and Gary R. Halford
Lewis Research Center
Cleveland, Ohio



National Aeronautics and
Space Administration
Office of Management
Scientific and Technical
Information Division

1989

Summary

The procedures are presented for characterizing an alloy and predicting cyclic life for isothermal and thermomechanical fatigue conditions by using the total strain version of Strainrange Partitioning (TS-SRP). Numerical examples are given. Two independent alloy characteristics are deemed important: *failure* behavior, as reflected by the inelastic strainrange versus cyclic life relations; and *flow* behavior, as indicated by the cyclic stress-strain-time response (i.e., the constitutive behavior). *Failure* behavior is characterized by conducting creep-fatigue tests in the strain regime, wherein the testing times are reasonably short and the inelastic strains are large enough to be determined accurately. At large strainranges, stress-hold, strain-limited tests are preferred because a high rate of creep damage per cycle is inherent in this type of test. At small strainranges, strain-hold cycles are more appropriate. *Flow* behavior is characterized by conducting tests wherein the specimen is usually cycled far short of failure and the wave shape is appropriate for the duty cycle of interest.

In characterizing an alloy pure fatigue, or PP, failure tests are conducted first. Then depending on the needs of the analyst a series of creep-fatigue tests are conducted. As many of the three generic SRP cycles are featured as are required to characterize the influence of creep on fatigue life (i.e., CP, PC, and CC cycles, respectively, for tensile creep only, compressive creep only, and both tensile and compressive creep). Any mean stress effects on life also must be determined and accounted for when determining the SRP inelastic strainrange versus life relations for cycles featuring creep. This is particularly true for small strainranges. The life relations thus are established for a theoretical zero mean stress condition.

Introduction

Strainrange Partitioning (SRP) (ref. 1) was formulated on an inelastic strainrange basis, wherein the cyclic life is a function of the type and magnitude of the inelastic strainrange at a specific temperature. This approach has worked well in the high-strain, short-life regime for which the inelastic strains are large enough to be determined accurately by analytical or experimental methods. Procedures for characterizing and predicting cyclic life in this strain regime are described in

reference 2. Limitations of the inelastic method to application in the low-strain regime were recognized soon after SRP was proposed (ref. 3).

In order to extend the method into the technologically important low-strain, long-life regime, where the inelastic strains are small and difficult to determine, it was necessary to consider the total strainrange rather than just the inelastic strainrange. Four publications have documented the evaluation of the total strain version of SRP (refs. 4 to 7). Formulating SRP on a total strain basis requires the determination of both the elastic and inelastic strainrange versus cyclic life relations for the time-independent PP cycle and as many of the three generic time-dependent SRP creep cycles as required. The inelastic strainrange versus cyclic life relations normally used in an SRP analysis are still required. The elastic strainrange versus life relations for cycles involving creep are influenced by temperature, hold time, wave shape, and how creep is introduced into the cycle (stress hold, strain hold, slow strain rate, etc.). This means, for example, that for a given imposed cycle at a specific temperature, the elastic line intercept (elastic strainrange at one cycle to failure) is a function of hold time.

In the first paper published on TS-SRP (ref. 4) the elastic line intercept was determined by using an empirical equation with constants determined from failure test data (i.e., inelastic strainrange versus life). Following this approach would require that failure testing be done in the low-strainrange, long-life regime in order to reduce extrapolation errors when predicting cyclic life. However, a serious engineering drawback of this approach is that such tests are quite expensive because they require excessively long times to conduct. Obviously it would be advantageous to be able to characterize an alloy without having to conduct lengthy failure tests.

Efforts to reduce failure testing requirements led to the development of the updated version of TS-SRP (ref. 5). This development is based on a relation between failure behavior and flow behavior (cyclic stress-strain response) and greatly reduces the time and cost of characterizing an alloy in the low-strain, long-life regime. Flow behavior is characterized from data obtained from tests wherein a specimen is cycled until the stress-strain hysteresis loop satisfies the criteria for stability. Thus the procedures for characterizing an alloy for TS-SRP are based on those used for the inelastic strainrange approach (refs. 1 and 2) with certain modifications and some additional nonfailure cyclic tests at low strain levels and long

times per cycle but relatively few cycles per test (i.e., far short of running to failure).

The TS-SRP method has been modified recently for predicting the lives of thermomechanical fatigue (TMF) cycles (refs. 7 and 8). Because little experimental verification is available to date for this modification, the emphasis in this report is on isothermal fatigue. Traditionally TMF resistance of materials has been estimated by using techniques developed for isothermal conditions, with cyclic life being predicted at the peak temperature of the cycle. However, this approach for predicting TMF life in the low-strain regime lacks both accuracy and generality as demonstrated in reference 9. That study has shown that the numerous methods proposed to date are ineffective, in general, in predicting TMF life. The extension of TS-SRP into the TMF regime represents one of the first rational approaches to be proposed for predicting thermal fatigue crack initiation life.

This report discusses in detail the steps required to characterize an alloy and to predict cyclic life in the low-strain regime when using the updated TS-SRP approach. Emphasis is placed on isothermal fatigue because the extension of the method to thermomechanical fatigue has yet to be verified.

Symbols

A, A'	general constant in empirical flow equations
B	intercept of elastic strainrange versus life relations
C	intercept of inelastic strainrange versus life relations
C'	intercept of equivalent inelastic line for combined creep-fatigue cycles
F	strain fraction
K	cyclic strain-hardening coefficient
k	mean stress correction term
N	number of applied cycles
V	ratio of mean to amplitude
t	hold time, sec
Δ	range of variable
ϵ	strain
σ	stress

Exponents:

b	power of cyclic life for elastic strainrange versus life relations
c	power of cyclic life for inelastic strainrange versus life relations
m	general power of time in empirical flow equations
n	cyclic strain-hardening exponent
α	power on total strainrange in empirical flow equations

Subscripts:

a	amplitude
c	compression
cc	creep strain in tension, creep strain in compression
cp	creep strain in tension, plastic strain in compression
el	elastic
f	failure
f_0	failure at zero mean stress
fm	failure with mean stress
in	inelastic
ij	PP, PC, CP, CC
m	mean
pc	plastic strain in tension, creep strain in compression
pp	plastic strain in tension, plastic strain in compression
t	tension
σ	stress

Isothermal cycle types:

BCCR	balanced cyclic creep rupture (PP + CC strainranges)
BHSC	balanced-hold strain cycle (PP + CC strainranges)
CCCR	compressive cyclic creep rupture (PP + PC strainranges)
CCDF	CC damage fraction
CHSC	compressive-hold strain cycle (PP + PC strainranges)
HRLC	high-rate load cycle (PP strainrange)
HRSC	high-rate strain cycle (PP strainrange)
PCDF	PC damage fraction
PPDF	PP damage fraction
TCCR	tensile cyclic creep rupture (PP + CP strainranges)
THSC	tensile-hold strain cycle (PP + CP strainranges)

Background

Strainrange Partitioning is based on the premise that cyclic life is a function of the inelastic strainrange and the type and relative amounts of time-independent strain (plasticity) and time-dependent strain (creep) present in a cyclic stress-strain hysteresis loop (ref. 1). Expressing SRP in terms of total strainrange does not change this premise.

In formulating the total strain version of SRP (TS-SRP) (refs. 4 and 5), we assumed that the inelastic and elastic failure lines for isothermal creep-fatigue cycles are parallel to the corresponding failure lines for pure fatigue (PP cycles) as shown in figure 1. This is not an arbitrary assumption. Our

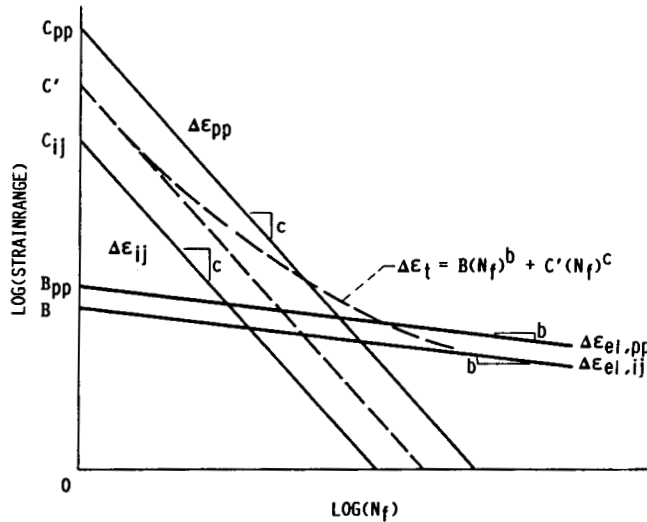


Figure 1.—Relation between total strainrange and life for creep-fatigue cycles. Inelastic line intercept C' is determined from equation (3) and elastic line intercept B is determined from equation (7).

experience with several alloys suggests that this is a reasonable assumption. Note also that the frequency-modified approach of Coffin (ref. 10) also assumes parallel inelastic lines and parallel elastic lines. The extension of TS-SRP into the TMF regime (ref. 7) retains this assumption of parallel lines. Limited data for Haynes 188 (ref. 11) and unpublished NASA data for B1900 + Hf suggest that this approach is realistic.

Analysis shows that there is a relationship between failure behavior and flow behavior. Failure behavior is described by the following equations:

$$\Delta\epsilon_{el} = B(N_{f0})^b \quad (1)$$

$$\Delta\epsilon_{in} = C'(N_{f0})^c \quad (2)$$

where

$$C' = \left[\sum F_{ij}(C_{ij})^{1/c} \right]^c \quad (3)$$

and the subscripts ij denote the type of cycle.

Equation (3) is derived from the interaction damage rule (IDR) (ref. 12) and the four generic SRP inelastic strainrange versus cyclic life relations for a "theoretical zero mean stress condition." In the past the inelastic line intercepts for creep cycles (C_{pc} , C_{cp} , and C_{cc}) have been taken to be independent of time. But recent developments (ref. 13) indicate that for 316 stainless steel at 816 °C they are time dependent, and procedures have been proposed for expressing the time dependencies analytically. The following discussion does not consider explicitly the time dependency of the inelastic lines, although it could be added if needed.

The four generic SRP life relations are

$$\Delta\epsilon_{in} = C_{ij}(N_{ij})^c \quad (4)$$

where $ij = pp, pc, cp, \text{ or } cc$. The IDR is written as follows:

$$\sum \left(\frac{F_{ij}}{N_{ij}} \right) = \frac{1}{N_{f0}} \quad (5)$$

Note that both PC and CP strainranges cannot occur in the same hysteresis loop. Equation (3) is obtained by using equation (4) to solve for N_{ij} and then substituting this term in equation (5). Flow behavior is described by

$$\Delta\epsilon_{el} = K_{ij}(\Delta\epsilon_{in})^n \quad (6)$$

where $n = b/c$.

Assuming that the inelastic and elastic failure lines for creep-fatigue cycles are parallel to the corresponding failure lines for PP cycles, it follows that the strain-hardening exponent n in equation (6) is a constant as shown in figure 2. For isothermal conditions the strain-hardening coefficient K_{ij} is a function of temperature, total strainrange, hold time, how creep is introduced into the cycle (stress hold, strain hold, etc.), and the strainrate-hardening characteristics of the alloy. For nonisothermal conditions K_{ij} is also a function of the maximum and minimum temperatures and the phase relation between strain and temperature.

The time-dependent behavior of the elastic line for creep cycles is shown in figure 3. Setting equation (1) equal to equation (6) and eliminating N_{f0} by using equation (2), we obtain the following equation relating flow and failure behavior:

$$B = K_{ij}(C')^n \quad (7)$$

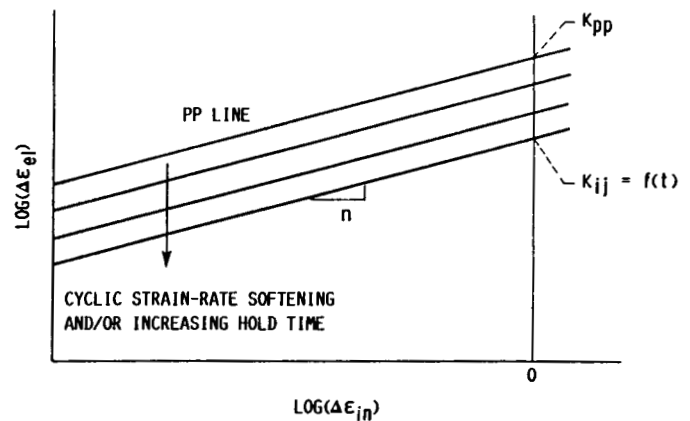


Figure 2.—Relation between inelastic and elastic strainranges for creep-fatigue cycles. Cyclic strain-hardening coefficient K_{ij} is a function of hold time and strain-rate-hardening characteristics of an alloy.

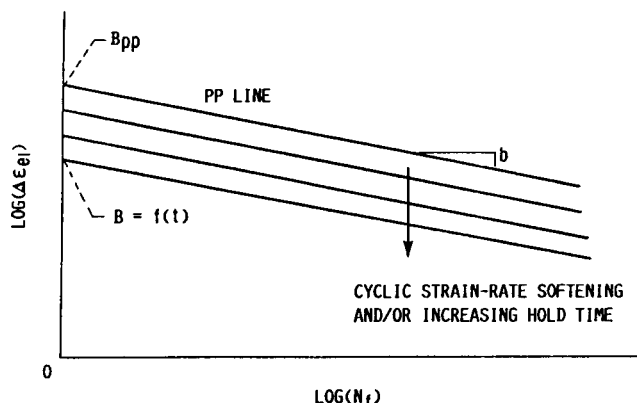


Figure 3.—Relation between elastic strainrange and life for creep-fatigue cycles. Variation in elastic line intercept is a function of hold time and strain-rate-hardening characteristics of an alloy.

The inelastic line intercepts C_{ij} , the exponent c , and the term C' are considered to be failure terms. The strain fractions F_{ij} , the cyclic strain-hardening coefficients K_{ij} , and the strain-hardening exponent n are considered to be flow terms. Thus the elastic line intercept B is determined by a combination of both flow and failure terms.

We are now in a position to establish a total strainrange versus life relation and thus predict life on a total strain basis. The total strainrange is the sum of the elastic and inelastic strainranges:

$$\Delta\epsilon_t = \Delta\epsilon_{el} + \Delta\epsilon_{in} \quad (8)$$

From equations (1) and (2) we obtain

$$\Delta\epsilon_t = B(N_{f0})^b + C'(N_{f0})^c \quad (9)$$

Earlier in this section we noted that SRP was originally formulated on an inelastic strain basis. Adding the elastic strain to the inelastic strain and formulating SRP on a total strain basis does not alter the basic premise that inelastic strains are always present, even in the nominally elastic region.

A schematic plot of equation (9) is shown in figure 1. Note that the solution of this equation gives the cyclic life for a theoretical zero mean stress condition N_{f0} . The final step in a life prediction is to adjust the computed life to account for any mean stress effects that may be present. In this paper the method of mean stress correction proposed by Halford and Nachtigall (ref. 14) is used. Note that the method given in reference 14 is for isothermal conditions, was developed for a specific nickel-based alloy, and may not apply to other alloys or even to other nickel-based alloys. The analyst must determine that the mean stress correction equation used is applicable to the alloy of interest. For TMF an alternative method is required since a mean stress can naturally develop because of the temperature dependency of the yield strength in tension and compression. A method for dealing with this

has been proposed in reference 9, but to date there has been no experimental verification.

The preceding analysis is easily extended to TMF with little modification. For purposes of discussion, consider an inphase tensile-hold strain cycle. In this type of cycle the temperature and strain vary in unison and the strain is held constant at maximum strain and maximum temperature. Since this cycle produces PP and CP inelastic strainranges, PP and CP life relations (eq. (4)) are required, and both relations must be for inphase cycling. Flow behavior is characterized by equation (6). With this information the inelastic line intercept C' and the elastic line intercept B are calculated from equations (3) and (7), respectively.

This approach is based on the assumption that the inelastic and elastic failure lines for creep-fatigue cycles are parallel to the respective lines for pure fatigue. Although this condition is known to exist for some materials, it may not always be a satisfactory assumption. An approach has been developed in reference 7 to deal with this and is contained in the appendix for the convenience of the reader.

In order to predict life on a total strain basis, it is necessary to determine the intercepts B and C' and the exponents b and c in equation (9). The approach taken to determine these values depends on what type of information is, or can be made, available. It is appropriate at this point to discuss the method of experimentally determining the failure terms b and c in equations (1) and (2), respectively, and the flow term n in equation (6). Equation (6) is obtained from equations (1) and (2), and $n = b/c$. The values of b and c are determined from PP failure tests. Typically the number of these tests is limited by economic considerations, and n will not be exactly equal to b/c because of the inherent variation in the data. A better estimate of n can be obtained by conducting additional PP flow tests, where the specimen is cycled just long enough for the stress-strain hysteresis loop to satisfy the criteria for stability. A method for determining these stability criteria is given in a later section. Adding these data to the PP failure data will give a better estimate of n in equation (6).

Three variants for predicting cyclic life with TS-SRP have been identified in reference 4 and are described here. Which variant is appropriate for use depends upon the extent of material property data that can be made available.

Variant 1

(a) Determine the SRP inelastic strainrange versus cyclic life relations and the PP elastic strainrange versus cyclic life relations from failure tests. As an alternative to measuring the inelastic strainrange versus cyclic life relations, they may be approximated by the empirical ductility-normalized SRP (DN-SRP) life relations proposed by Halford and Saltsman (ref. 15). The DN-SRP approach requires plastic and creep ductility information to be calculated from reduction-of-area data obtained from tensile and creep-rupture tests, respectively, at

the temperature of interest. DN-SRP relations have as yet to be proposed for nonisothermal fatigue.

(b) Calculate the cyclic strain-hardening coefficient K_{ij} , the cyclic strain-hardening exponent n , and the strain fractions F_{ij} by using an appropriate constitutive flow model for which the material constants are known. If the DN-SRP life relations are used, the cyclic strain-hardening exponent n should be determined from flow tests and the slope of the PP elastic line calculated ($b = nc$).

(c) The elastic line intercept B can now be calculated by using equation (7) and the preceding information.

(d) Determine the total strainrange versus life curve for the case in question (fig. 1). Enter the curve at the appropriate total strainrange and determine the cyclic life for the theoretical zero mean stress condition. In this report we have used the inversion method of Manson and Muralidharan (ref. 16) to solve equation (9). This life is then adjusted to account for mean stress effects as discussed in a later section.

Variant 2

(a) Determine the SRP inelastic strainrange versus life relations and the PP elastic strainrange versus life relations from failure tests.

(b) Determine the elastic intercept B by using the empirical equation of Halford and Saltsman (ref. 4). The constants in this equation are determined from failure data. Failure tests should be performed at the lower strain ranges to reduce extrapolation errors. The applicability of this means of determining B for nonisothermal fatigue has not been examined.

(c) Measure strainranges (elastic and inelastic) and stresses from failure tests and extrapolate to lower strainranges by using empirical equations.

(d) Determine cyclic life from step (d) of variant 1.

Variant 3

(a) Same as step (a) of variant 1. Additional PP flow tests are conducted to obtain an accurate estimate of the cyclic strain-hardening exponent n .

(b) Conduct flow tests for creep-fatigue cycles of interest and determine the necessary empirical correlations describing flow behavior. If failure data are lacking and the DN-SRP relations are used, PP flow tests must be done to determine the strain-hardening exponent n . The slope of the PP elastic line can then be calculated ($b = nc$).

(c) Use equation (7) to calculate the elastic line intercept B . Determine the strain-hardening coefficient K_{ij} and the strain fractions F_{ij} from the correlations obtained in step (b).

(d) Determine cycle life from step (d) of variant 1.

Although variant 1 is the most general procedure, it is not a particularly viable option at this time because of the lack of data to reliably evaluate constitutive flow models in the low-

strain regime. Variant 2 was used in the original TS-SRP paper (ref. 4) and relies entirely on failure data for determining the required equation constants. Variant 3 (ref. 5) represents a middle ground between variants 1 and 2. Inelastic strainrange versus cyclic life relations based on failure data are necessary for reliable life predictions, but preliminary predictions can be made for isothermal conditions by using the DN-SRP relations and information obtained from flow tests.

The Walker constitutive model (ref. 17) was used to generate the isothermal flow information needed to identify *trends* in material behavior. From this information we were able to show that the appropriate flow terms could be correlated by using a simple power law. This same power law was also used successfully to correlate computer-generated nonisothermal flow information (ref. 7).

$$y = A(t)^m \quad (10)$$

The dependent variable y represents several flow variables as discussed below, and t is the hold time per cycle. Results from the Walker flow model show that A is a function of total strainrange and the exponent m can be taken as a constant for a given correlation. Equation (10) is shown schematically in figure 4. It has been found that the intercept A can be correlated with total strainrange by another power law as shown below and in figure 5.

$$A = A'(\Delta\epsilon_t)^\alpha \quad (11)$$

Thus

$$y = A'(\Delta\epsilon_t)^\alpha(t)^m \quad (12)$$

The dependent variable y is now a function of two independent variables, $\Delta\epsilon_t$ and t . If both sides of equation (12) are divided by $(\Delta\epsilon_t)^\alpha$, the family of lines shown schematically in figure 4 reduces to a single line as shown in figure 6. The values of A' , α , and m must be determined for each flow variable (i.e., K_{ij} , F_{ij} , $\Delta\epsilon_{el}$, etc.).

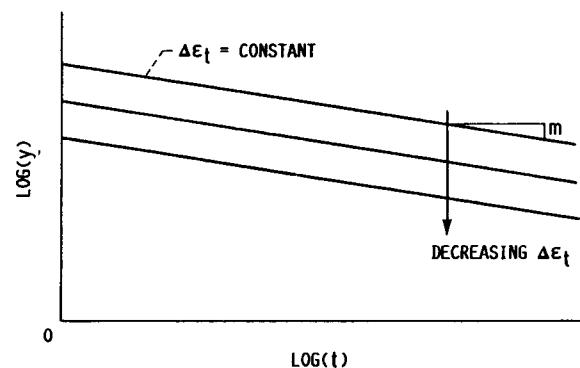


Figure 4.—Power law used to correlate flow data. Lines are parallel, and intercept A at $t = 1$ sec is a function of total strainrange.

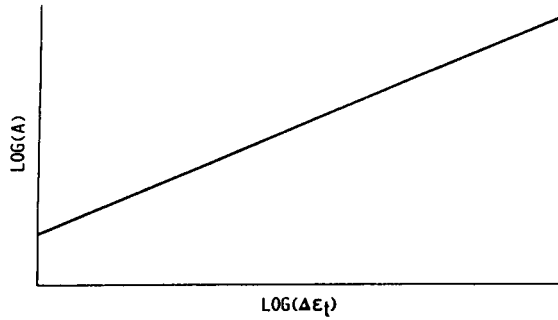


Figure 5.—Relation between intercept of power law equation and total strainrange.

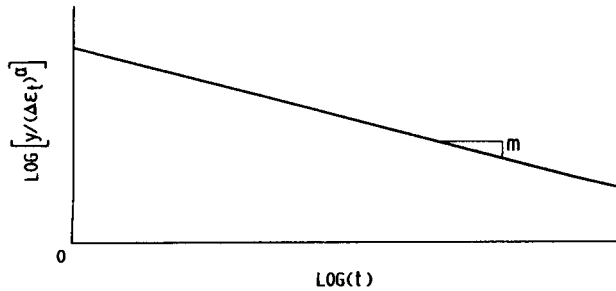


Figure 6.—Power law normalized on total strainrange raised to suitable power reducing family of lines shown in figure 4.

The dependent variable in equation (12) represents the several flow variables listed here. The first two are used to determine the coefficients B and C' in equation (9), and the rest are used to determine the mean stress correction for both isothermal (ref. 14) and nonisothermal (ref. 9) conditions.

K_{ij} versus hold time
 F_{ij} versus hold time

} To determine B and C'

$\Delta\epsilon_{el}$ versus hold time
 $\Delta\sigma$ versus hold time
 σ_c versus hold time
 σ_t versus hold time

} To determine mean stress correction

The procedures for characterizing the failure and flow behavior of an alloy are discussed in detail in the following section. The example alloy used was AF2-1DA at 760 °C. Ideally the same heat of alloy should be used. However, we were obliged to depend on published data obtained from different heats. Also, the flow response was determined by using flow data from failure tests. This was done out of necessity because specimens were no longer available for additional flow testing.

Alloy Characterization

Failure Relations

The testing techniques given in reference 2 are used to determine the four generic SRP inelastic strainrange versus life relations. However, some additional steps must be taken to obtain the life relations for the TS-SRP approach as explained later in this section. The method for determining the required life relations is illustrated by using data taken from reference 14 and listed in table I. The definition of failure for these relations depends on the application and the mechanical properties of the alloy. Probably the most common definition of failure is complete separation of the specimen as in reference 14. Other definitions could be surface crack size as in reference 6 or drop in the tensile peak load as in reference 11.

The pure fatigue, or PP, tests are conducted first since this life relation must be known in order to determine the life relations for cycles containing creep. These tests are conducted at a zero mean strain condition to minimize mean stress effects on cyclic life. Most alloys develop a small negative mean stress under this type of loading, and its effect is usually neglected. The elastic strainrange versus life and inelastic strainrange versus life relations are now determined for this nominal zero mean stress condition. A log-log linear regression of the appropriate data in table I performed by using equations (1) and (4) yields the following, where the strainranges $\Delta\epsilon_{el}$ and $\Delta\epsilon_{in}$ are the independent variables and cyclic life N_{pp} is the dependent variable:

$$\Delta\epsilon_{el} = 0.022(N_{pp})^{-0.117} \quad (13)$$

$$\Delta\epsilon_{in} = 0.100(N_{pp})^{-0.637} \quad (14)$$

These correlations are shown in figure 7.

Additional PP tests should now be conducted to determine the effects of mean stress on life because mean stress effects must be accounted for when determining the life relations for cycles involving creep. This point is frequently overlooked by users of SRP as well as other life prediction methods. Note that a cycle featuring compression creep will usually have a tensile mean stress, and a cycle featuring tensile creep will usually have a compressive mean stress. A tensile mean stress will generally reduce life, and a compressive mean stress will generally increase life. Failure to account for mean stress effects on life can produce misleading results.

Generally each alloy must be considered separately when evaluating mean stress effects. The procedure given in reference 14 was developed with data for the nickel-based alloys AF2-1DA and IN-100. When evaluating the effects of mean stress on B1900 + Hf (ref. 6), also a nickel-based alloy, it was found that tensile mean stresses had little or no effect on life but that compressive mean stresses increased life.

TABLE I.—DATA USED TO ESTABLISH SRP INELASTIC STRAIN RANGE VERSUS LIFE RELATIONS

[Alloy, AF2-1DA; temperature, 760 °C; data from ref. 14.]

(a) Rate data and stresses

Specimen	Test type ^a	Rate data (half-life values)				Stresses (half-life values), MPa				Cyclic strain hardening ^b				
		Frequency, Hz	Strain rate in tension and compression, percent/sec	Hold time, sec		Maximum tension	Maximum compression	Maximum range	Ratio of mean stress to stress amplitude					
				Tension	Compression									
AF-11	HRSC	0.5	0.024	0	0	1236.0	1336.0	2572.0	-0.039	S				
AF-15	↓	↓	.015	↓	↓	970.0	1021.0	1991.0	-.026	↓				
AF-21			.011			756.0	792.0	1548.0	-.023					
AF-6			.010			767.0	780.0	1547.0	-.008					
AF-9			.0089			688.0	689.0	1377.0	-.001					
AF-33			.0082			674.0	676.0	1350.0	-.001					
AF-XX			.84			689.5	689.5	1379.0	0					
AF-10			.0082			607.0	605.0	1212.0	.002					
AF-3			.0066			564.0	560.0	1124.0	.004					
AF-42			CCCR		.017	.00053	1470.0	965.0	699.0		1664.0	.160	H	
AF-26			↓		↓	.014	↓	285.0	938.0		721.0	1659.0	.131	↓
AF-34	.032	.00070		428.0		983.0		626.0	1609.0	.222				
AF-36	.050	.00094		72.0		878.0		623.0	1501.0	.170				
AF-40	.059	.00084		327.0		856.0		347.0	1203.0	.423				
AF-43	.036	.00056		76.0		768.0		546.0	1314.0	.169				
AF-47	TCCR	.1		.0029		577.0		0	701.0	1154.0	1855.0	-.244	S	
AF-5	TCCR	.1		.0011		130.0		0	582.0	1028.0	1610.0	-.277	S	
AF-27	TCCR	.074		.0011		46.0		0	440.0	865.0	1305.0	-.326	S	
AF-25	BCCR	.050	.0015	744.0	2220.0	734.0	734.0	1468.0	0	--				
AF-41	BCCR	.1	.0022	212.0	569.0	665.0	674.0	1339.0	-.007	S				
AF-28	BCCR	.1	.0014	42.0	67.0	605.0	512.0	1117.0	.083	S				

^aSee symbol list.^bS = soften; H = harden.

(b) Strains and failure data

Specimen	Strainranges (half-life values), percent							Cycles to failure, N_f	Time to fail, hr
	Total	EL	IN	PP	PC	CP	CC		
AF-11	2.388	1.492	0.896	0.896	0	0	0	43	0.02
AF-15	1.523	1.155	.368	.368	↓	↓	↓	200	.11
AF-21	1.052	.898	.154	.154				756	.42
AF-6	1.002	.898	.104	.104				1 322	.71
AF-9	.888	.799	.089	.089				2 695	1.50
AF-33	.815	.783	.032	.032				5 745	3.20
AF-XX	.837	.800	.037	.037				4 205	2.24
AF-10	.721	.703	.018	.018				25 433	13.60
AF-3	.663	.652	.011	.011				59 121	31.60
AF-42	1.589	.966	.623	.269	.354			62	26.30
AF-26	1.265	.962	.303	.151	.152			226	20.20
AF-34	1.124	.933	.191	.083	.108			345	42.50
AF-36	.943	.871	.072	.027	.045	741	18.90		
AF-40	.752	.698	.054	.022	.032	1 285	119.90		
AF-43	.807	.762	.045	.016	.029	1 400	40.50		
AF-47	1.444	1.076	.368	.160	0	.208	103	16.90	
AF-5	1.091	.934	.157	.082	↓	.075	458	19.20	
AF-27	.805	.757	.048	.024	↓	.024	8 805	139.30	
AF-25	1.492	.851	.641	.160	↓	0	.481	114	93.80
AF-41	1.112	.777	.335	.096	↓	0	.239	176	38.20
AF-28	.718	.648	.070	.026	↓	0	.044	3 550	107.00

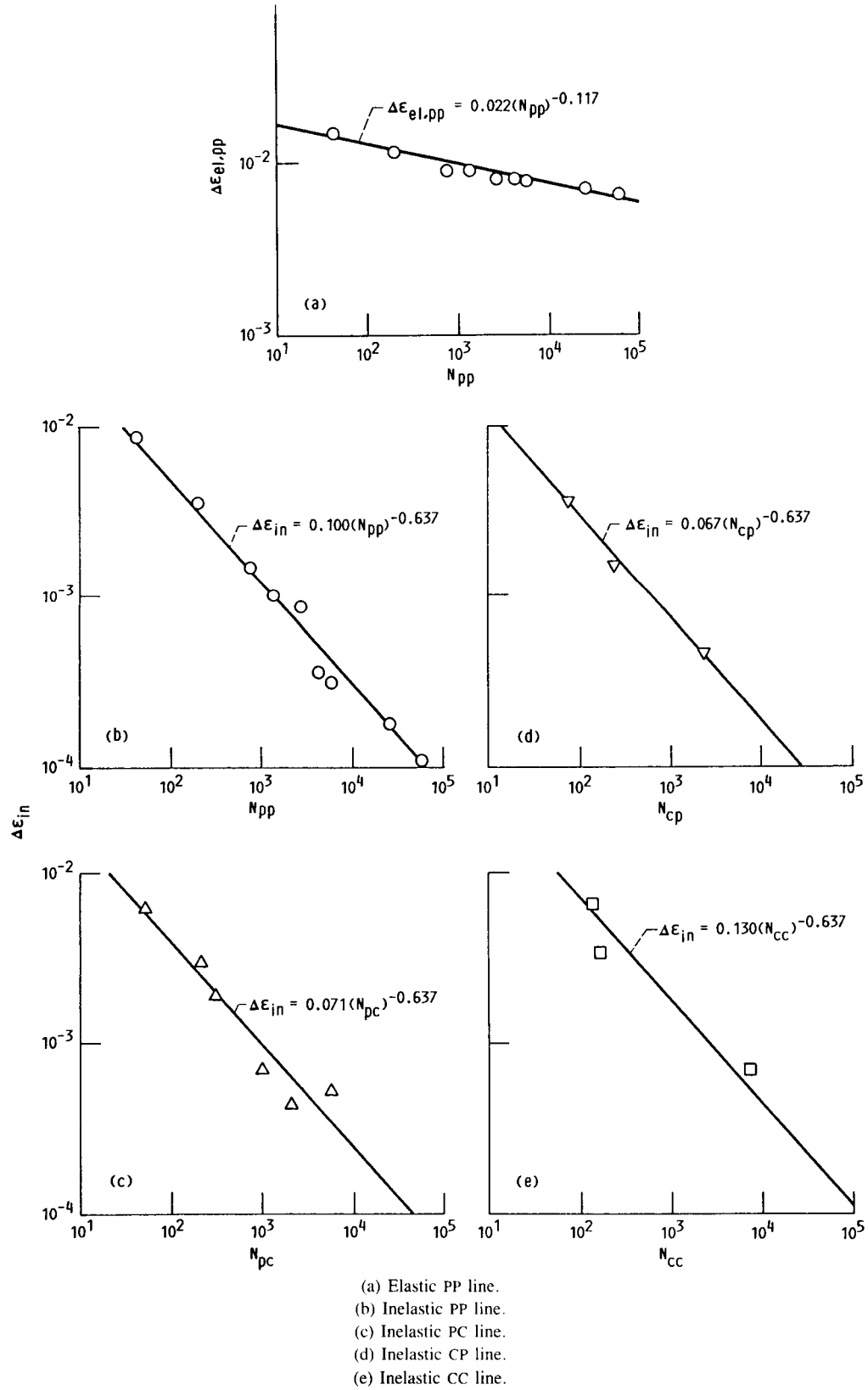


Figure 7.—Failure relations for zero mean stress condition: alloy, AF2-1DA, temperature, 760 °C. (Data from ref. 14.)

Data from PC, CP, and CC tests can now be analyzed and the appropriate inelastic strainrange versus life relations determined. It is strongly recommended that stress-hold tests be conducted to determine these relations rather than strain-hold tests. The stress-hold test imparts far more creep damage to the material than the strain-hold test, and uncertainty in the life relations is reduced. We have found the inelastic strainrange versus life relations for the creep cycles to be insensitive to waveform. Thus the life relations obtained from the stress-hold tests can be used to predict the life in any other cycle involving creep.

Introducing creep into the fatigue cycle generally reduces life. This reduction in life may not be due entirely to creep effects. Oxidation and other environmental factors can cause a degradation of the material that in some cases may be more significant than creep effects. But for simplicity, we combine all of these effects under the term "creep damage."

The steps involved in determining the inelastic strainrange versus life relations for creep cycles are illustrated with an example that uses data from table I for alloy AF2-1DA. We shall assume that the PC life relation is to be determined. First, the observed life N_{fm} is corrected to a theoretical zero mean stress life N_{f0} . As noted earlier, the method given in reference 14 is used here, and the definition of failure is complete separation of the specimen. Note that a method suitable for one definition of failure may not be suitable for other definitions of failure.

$$N_{f0} = \left[N_{fm}^{|b|} + kV_{\sigma} \right]^{1/|b|} \quad (15)$$

and

$$k = \exp \left[-70 \left(\frac{\Delta \epsilon_{in}}{\Delta \epsilon_{el}} \right)^2 \right] \quad (16)$$

With the observed lives adjusted for mean stress effects by using equation (15), we can now use the IDR (eq. (5)) to determine the PC life relation.

$$\frac{F_{pp}}{N_{pp}} + \frac{F_{pc}}{N_{pc}} = \frac{1}{N_{f0}} \quad (17)$$

Rewriting equation (17) gives

$$\frac{F_{pp}(N_{f0})}{N_{pp}} + \frac{F_{pc}(N_{f0})}{N_{pc}} = 1 \quad (18)$$

where the first term on the left side is the PP damage fraction (PPDF) and the second term is the PC damage fraction (PCDF). Thus

$$\text{PPDF} + \text{PCDF} = 1 \quad (19)$$

When determining the life relation for a cycle containing creep, the creep damage must be large enough that a valid representation of this type of behavior is obtained. Thus in this example the dominant damage in the cycle must be due to a PC strainrange component. This is accomplished when PCDF is ≥ 0.50 as recommended in reference 2. It is also suggested that the strainrange component of interest be the dominant component of the inelastic strainrange ($F_{pc} \geq 0.50$ for this example).

Failure to observe these criteria along with not correcting the observed life for mean stress effects can result in life relations of questionable validity and in some cases the total inability to determine the desired life relation. Failure to conduct the proper tests and/or account for mean stress effects can cause the PPDF in equation (19) to be greater than unity, and hence a meaningless negative life would be calculated. Solving for N_{pc} in equation (18) gives

$$N_{pc} = \frac{F_{pc}(N_{f0})}{1 - \text{PPDF}} \quad (20)$$

As an example, we shall use the data for specimen AF-43 from table I. This point was selected because the total strainrange is low (0.00807) and the effect of mean stress on life is significant. The appropriate values are

$$\Delta \epsilon_{in} = 0.00045$$

$$\Delta \epsilon_{pc} = 0.00029$$

$$\Delta \epsilon_{el} = 0.00762$$

$$V_{\sigma} = 0.169$$

$$N_{fm} = 1400 \text{ cycles}$$

$$|b| = 0.117 \text{ (from eq. (13))}$$

From equation (16)

$$k = \exp \left[-70 \left(\frac{0.00045}{0.00762} \right)^2 \right] = 0.783$$

The theoretical zero mean stress life is calculated from equation (15).

$$N_{f0} = [1400^{0.117} + 0.783(0.169)]^{1/0.117} = 2243 \text{ cycles}$$

The strain fractions F_{pc} and F_{pp} are

$$F_{pc} = \frac{0.00029}{0.00045} = 0.644$$

Since $\sum F_{ij} = 1.0$,

$$F_{pp} = 1.0 - 0.644 = 0.356$$

Solving for N_{pp} by using equation (14) gives

$$N_{pp} = \left(\frac{0.100}{0.00045} \right)^{1/0.637} = 4832 \text{ cycles}$$

We can now calculate the PP damage fraction (PPDF) in equation (19) and solve for the pure PC life, N_{pc} . This is the life that would result from an inelastic strainrange of 0.00045 if the PP strain component were not present (i.e., $F_{pc} = 1.0$). Solving for the PP damage fraction by using the first term in equation (18) gives

$$\text{PPDF} = \frac{0.356(2243)}{4832} = 0.1653$$

Since $\text{PPDF} + \text{PCDF} = 1.0$, $\text{PCDF} = 0.8347$. This is well in excess of the recommended minimum value of 0.50 and clearly illustrates the damaging nature of the stress-hold wave shape. Solving for N_{pc} by using equation (20) gives

$$N_{pc} = \frac{0.664(2243)}{1 - 0.1653} = 1784 \text{ cycles}$$

When all of the PC data are analyzed in the preceding manner, the inelastic strainrange versus life relation is determined in the same manner as the PP life relation. This results in the following equation:

$$\Delta\epsilon_{in} = 0.129(N_{pc})^{-0.718} \quad (21)$$

In the current variants of the TS-SRP approach, the inelastic strainrange versus life relations for creep cycles are assumed to be parallel to the PP line, so the constants in equation (21) must be adjusted accordingly. This is done by forcing a line through the centroid of the data parallel to the PP line. This results in the following equation:

$$\Delta\epsilon_{in} = 0.071(N_{pc})^{-0.637} \quad (22)$$

Since equation (21) is log-log linear, logarithmic values must be used in determining the centroid. Thus

$$\overline{\Delta\epsilon_{in}} = 10 \exp \left[\frac{\sum \log (\Delta\epsilon_{in})}{\text{no. of points}} \right] \quad (23)$$

$$\overline{N_{pc}} = 10 \exp \left[\frac{\sum \log (N_{pc})}{\text{no. of points}} \right] \quad (24)$$

Obviously equation (22) could have been solved without a formal regression analysis by simply determining the centroid

of the data and then calculating the value of C_{pc} from the known value of c (-0.637).

The procedure for determining the CP and CC life relations is identical to the preceding example. However, some CC tests generally would have a PC or CP strain component (in addition to a PP component) in the stress-strain hysteresis loop, and this must be taken into account when determining the pure CC life, N_{cc} . For the sake of discussion assume that a PC strain component is present. (Unfortunately, none of the BCCR data in table I have a PC strain component, so a numerical example cannot be given.) The inelastic strainrange will have the following components:

$$\Delta\epsilon_{in} = \Delta\epsilon_{pp} + \Delta\epsilon_{cc} + \Delta\epsilon_{pc} \quad (25)$$

The IDR for this type of cycle is written as

$$\frac{F_{pp}(N_{f0})}{N_{pp}} + \frac{F_{cc}(N_{f0})}{N_{cc}} + \frac{F_{pc}(N_{f0})}{N_{pc}} = 1 \quad (26)$$

or

$$\frac{F_{cc}(N_{f0})}{N_{cc}} = 1 - \text{PPDF} - \text{PCDF} \quad (27)$$

where the term on the left side of this equation is the CC damage fraction (CCDF). Solving for N_{cc} gives

$$N_{cc} = \frac{F_{cc}(N_{f0})}{1 - \text{PPDF} - \text{PCDF}} \quad (28)$$

If a CC test contains a PC (or CP) strain component, the PC (or CP) damage fraction should be determined by using the regressed strainrange versus life relation. Thus in this example equation (21) rather than equation (22) would be used to determine the PC damage fraction in equation (27). This is done because the regression line better represents the limited data available for determining the life relations.

The CP, PC, and CC life relations for AF2-1DA determined by these procedures are shown in figure 7. Note that the equation constants differ slightly from those reported earlier (refs. 4, 5, and 14), where the regression lines were forced to have an exponent of 0.600.

The preceding discussion detailed the steps involved in determining the inelastic strainrange versus life relations required for TS-SRP. The steps are essentially the same as in reference 2 with two exceptions: (1) the effect of mean stress on cyclic life is accounted for, and (2) the PC, CP, and CC life relations are forced to be parallel to the pure fatigue, or PP, line.

The procedure for determining the inelastic strainrange versus life relations is summarized as follows:

(1) Conduct pure fatigue, or PP, tests at zero mean strain and determine the elastic strainrange versus life and inelastic

strainrange versus life relations for the nominal zero mean stress condition. Conduct additional PP tests to determine the effects of mean stress life on cyclic life. Do not use these additional data to determine the PP failure line.

(2) Conduct creep-fatigue tests for the cycle types of interest (PC, CP, and CC). Stress-hold, strain-limited tests are preferred because they cause the most creep damage. The inelastic strainrange versus life relations are relatively insensitive as to how creep is introduced into the cycle (stress hold, strain hold, etc.). Therefore the life relations obtained with these data will be valid for all other creep-fatigue cycles of the same type.

(3) Determine the generic inelastic strainrange versus life relations for creep cycles by using the interaction damage rule (IDR). The observed cyclic lives of the tests used to determine these life relations *must* be corrected to a theoretical zero mean stress condition prior to determining the life relations. The life lines obtained from a regression analysis are then rotated about the centroid of the data and made parallel to the PP line.

(4) It is recommended that the creep damage fraction be ≥ 0.50 for the tests used to determine the PC, CP, and CC life relations. However, this criterion may be relaxed when data are limited. For example, only three data points are available to determine the CC life relation in figure 7. The CC damage fraction (CCDF) for one of these tests is only 0.387. The damage fraction criterion was relaxed and this point was included in the regression analysis. When the regression line was rotated to become parallel to the PP line, the resulting value of C_{cc} was 0.13. This is essentially equal to the intercept of the PP line. Therefore the CC line was made to coincide with the PP line. For most alloys the PC, CP, and CC life lines will be below the PP line. However, this is not a requirement for SRP. Creep has been known to enhance the fatigue life of some alloys (e.g., IN-792 + Hf, ref. 18). In such cases the life relations for cycles with creep would be above the PP line.

(5) The inelastic strainrange versus cyclic life relations determined in the preceding steps are for a theoretical zero mean stress condition.

Flow Relations

As noted earlier the intercepts B and C' in equation (9) are time dependent, and this time dependency is determined by the flow or stress-strain-time response of the material. The time dependency must be determined for a particular duty cycle. The flow response of an alloy for a particular cycle is determined by cycling a test specimen until the stress-strain hysteresis loop satisfies the criteria for stability. These criteria are influenced by the mechanical properties of the alloy, the temperature, and the type of cycle.

Our limited experience suggests that criteria based on life fraction would be more appropriate than those based on stress range or stress amplitude. With those criteria the specimen is cycled for a specified fraction of its estimated failure life

($N/N_{fm} = \text{a constant}$). The value of this constant will vary with the material, the temperature, and the type of cycle. An initial value of 0.10 to 0.15 is suggested in order to minimize test time and damage to the specimen so that it can be used for additional tests. As an example, assume that we must characterize the flow response of a CP duty cycle. The first step is to obtain a method for determining N_{fm} for this cycle. This is done by using the CP data obtained from the failure tests, plotting total strainrange $\Delta\epsilon_t$ versus observed life N_{fm} , and extrapolating these data to the low-strainrange regime. If a flow test on a material with a total strainrange of 0.008 is to be conducted and the estimated life from the preceding extrapolation is 1000 cycles, the flow test would be run for 100 to 150 cycles.

Flow testing should be done at several strain levels, and in particular at strain levels lower than those used for failure testing. A practical lower limit is dictated by the ability to accurately measure the appropriate strains and stresses in the hysteresis loop.

In our previous work (ref. 5) the exponent α in equation (12) was determined by trial and error. Rewriting equation (12) as

$$\frac{y}{(\Delta\epsilon_t)^\alpha} = A'(t)^m \quad (29)$$

normalizes the dependent variable y and makes it a function of only one variable, t . The constants A' and m can be determined by a simple log-log linear regression analysis.

The constants A' , α , and m in equation (12) can also be determined in a more direct manner. Since the equation is log-log linear, the constants can be determined by a multiple linear regression analysis. We shall use this approach in the following discussion.

For purposes of discussion let us assume that it is necessary to predict the cyclic life of a component that will experience strain-hold duty cycles. For a given alloy and temperature the constants A' , α , and m in each flow relation are dependent on wave shape. Thus it is necessary to use data obtained from strain-hold tests to determine the flow correlations. This is in contrast to the inelastic strainrange versus life relations, which are insensitive to wave shape. The data used here are for the alloy AF2-1DA (ref. 19) and are given in table II. These data were also used in reference 5. Data from flow tests are not available, so we are obliged to use failure data to obtain these correlations. The flow correlations are discussed in the sequence given in the section "Background." Unfortunately there are not sufficient data to determine the CC flow correlations.

Correlation between elastic and inelastic strainranges.—

This correlation is determined first because the cyclic strain-hardening exponent n is required to determine both the elastic line intercept B (eq. (7)) and the cyclic strain-hardening coefficient correlation K_{ij} for creep cycles. The value of n is determined from equation (6) and $\Delta\epsilon_{el} - \Delta\epsilon_{in}$ data obtained

TABLE II.—DATA USED TO ESTABLISH FLOW RELATIONS FOR STRAIN-HOLD CYCLES

[Alloy, AF2-1DA; temperature, 760 °C; data from ref. 19.]

(a) Rate data and stresses

Specimen	Test type ^a	Rate data (half-life values)				Stresses (half-life values), MPa						Cyclic strain hardening ^b
		Frequency, Hz	Strain rate in tension and compression, percent/sec	Hold time, sec		Maximum tension	Maximum compression	Maximum range	Relaxation		Ratio of mean stress to stress amplitude	
				Tension	Compression				Tension	Compression		
7	HRSC	0.50	1.5	0	0	1077.9	1130.6	2208.5	0	0	-0.024	H
12	↓	↓	1.1	↓	↓	944.9	1026.3	1971.2	↓	↓	-.041	H
9	↓	↓	.93	↓	↓	835.4	895.2	1730.6	↓	↓	-.035	S
10	↓	↓	.72	↓	↓	638.8	747.8	1386.5	↓	↓	-.079	↓
13	↓	↓	.65	↓	↓	633.7	557.1	1190.8	↓	↓	-.064	↓
14	↓	↓	.50	↓	↓	447.6	526.6	974.2	↓	↓	-.081	↓
16	THSC	.033	1.2	30.0	↓	997.0	1221.8	2218.7	166.7	↓	-.101	H
17	↓	.031	1.0	30.0	↓	878.0	1144.2	2202.2	78.9	↓	-.132	H
18	↓	.031	.75	30.0	↓	616.0	923.6	1539.6	14.3	↓	-.200	S
19	↓	.0082	1.2	120.0	↓	842.9	1070.5	1913.3	197.2	↓	-.119	H
20	↓	.0082	1.0	120.0	↓	740.9	1001.1	1740.9	134.4	↓	-.149	S
21	↓	.0082	.77	120.0	↓	564.3	830.5	1394.8	43.0	↓	-.191	↓
24	↓	.0011	1.2	900.0	↓	860.2	1264.2	2124.3	225.9	↓	-.190	↓
23	↓	.0011	1.0	900.0	↓	731.6	1211.4	1942.9	143.4	↓	-.247	↓
26	↓	.0011	.75	900.0	↓	417.9	765.3	1183.1	48.4	↓	-.294	↓
27	CHSC	.031	1.2	0	30.0	999.0	937.0	1936.0	0	134.4	-.032	↓
28	↓	.031	1.0	↓	30.0	911.2	840.8	1752.0	↓	84.3	-.040	↓
30	↓	.031	.51	↓	30.0	592.3	368.9	961.1	↓	9.0	-.232	H
31	↓	.0082	.53	↓	120.0	649.2	348.6	997.7	↓	15.9	-.301	↓
33	↓	.0082	1.2	↓	120.0	1081.8	968.8	2050.5	↓	185.2	-.055	↓
34	↓	.0082	1.0	↓	120.0	938.4	771.6	1709.9	↓	104.0	-.098	↓
35	↓	.0011	1.2	↓	900.0	1095.6	884.6	1980.2	↓	220.5	-.107	↓
36	↓	.0011	1.0	↓	900.0	992.5	682.3	1674.7	↓	120.1	-.185	S
47	↓	.0011	.75	↓	900.0	853.6	470.2	1323.8	↓	35.9	-.290	H
38	BHSC	.016	1.2	30.0	30.0	990.8	977.0	1967.8	152.4	148.8	-.007	H
39	BHSC	.016	1.0	30.0	30.0	849.1	884.9	1734.0	100.4	100.4	-.021	S
41	BHSC	.016	.50	30.0	30.0	422.7	535.7	958.4	16.1	16.1	-.118	H
45	TCCR	.00084	1.2	1 192.0	0	617.1	1074.9	1692.0	0	0	-.271	↓
48	↓	.0088	1.0	112.0	↓	620.5	983.2	1603.8	↓	↓	-.226	↓
49	↓	.0039	.75	257.0	↓	482.2	778.8	1256.9	↓	↓	-.236	↓
51	↓	.00052	.50	1 939.0	↓	310.3	602.6	912.9	↓	↓	-.320	--
52	CCCR	.00011	1.2	0	8 760.0	1092.9	620.6	1713.4	↓	↓	.276	S
61	CCCR	.0021	1.0	0	473.0	1018.4	622.6	1641.0	↓	↓	.241	H
65	BCCR	.00024	.00024	4 225.0	4 225.0	620.6	620.6	1241.1	↓	↓	0	--
72	BCCR	.000021	.000012	46 729.0	46 729.0	620.9	607.1	1228.0	↓	↓	.011	H
73	CCCR	.0028	.75	0	357.0	820.8	449.6	1320.3	↓	↓	.281	↓
55	HRSC	.50	.82	↓	0	1082.8	342.4	1425.1	↓	↓	.520	↓
53	↓	↓	.50	↓	↓	807.4	87.6	895.0	↓	↓	.804	↓
3	↓	↓	.80	↓	↓	822.8	493.4	1316.2	↓	↓	.250	↓
4	↓	↓	1.0	↓	↓	919.8	758.4	1678.2	↓	↓	.096	↓
5	↓	↓	1.5	↓	↓	1087.4	1059.0	2146.4	↓	↓	.013	↓

^aSee symbol list.^bS = soften; H = harden.

TABLE II.—CONCLUDED
(b) Strains and failure data

Specimen	Strainranges (half-life values), percent							Cycles to failure, N_f	Time to fail, hr
	Total	EL	IN	PP	PC	CP	CC		
7	1.485	1.150	0.335	0.335	0	0	0	114	0.07
12	1.260	1.085	.175	.175	↓	↓	↓	321	.18
9	1.000	.930	.070	.070	↓	↓	↓	678	.38
10	.735	.720	.015	.015	↓	↓	↓	4 957	2.75
13	.650	.645	.005	.005	↓	↓	↓	27 087	15.05
14	.500	.495	.005	.005	↓	↓	↓	196 657	109.30
16	1.245	1.007	.238	.145	↓	.093	↓	395	3.52
17	1.025	.910	.115	.071	↓	.044	↓	928	8.25
18	.750	.722	.028	.020	↓	.008	↓	17 400	154.70
19	1.200	.995	.205	.095	↓	.110	↓	312	10.60
20	1.030	.892	.138	.063	↓	.075	↓	812	27.50
21	.768	.713	.055	.031	↓	.024	↓	5 380	182.30
24	1.210	.940	.270	.144	↓	.126	↓	197	49.40
23	1.000	.850	.150	.070	↓	.080	↓	716	179.40
26	.750	.690	.060	.033	↓	.027	↓	3 522	882.50
27	1.215	1.030	.185	.110	.075	0	↓	270	2.25
28	1.015	.925	.090	.043	.047	↓	↓	880	7.33
30	.505	.500	.005	0	.005	↓	↓	31 174	259.80
31	.525	.515	.010	.001	.009	↓	↓	22 163	751.10
33	1.200	.950	.250	.145	.105	↓	↓	185	6.30
34	1.005	.895	.110	.052	.058	↓	↓	399	13.50
35	1.200	.930	.270	.147	.123	↓	↓	179	44.90
36	1.015	.885	.130	.063	.067	↓	↓	285	71.40
47	.750	.715	.035	.015	.020	↓	↓	1 156	289.70
38	1.210	.970	.240	.155	0	.002	.083	96	1.65
39	1.000	.845	.155	.099	↓	0	.056	771	13.30
41	.500	.490	.010	.001	↓	0	.009	25 919	446.40
45	1.200	.905	.295	.085	↓	.210	0	263	87.20
48	1.000	.900	.100	.050	↓	.050	↓	836	26.40
49	.750	.725	.025	.005	↓	.020	↓	7 407	532.50
51	.500	.485	.015	0	↓	.015	↓	c1 287	693.30
52	1.200	.925	.275	.100	.175	0	↓	69	18.25
61	1.000	.895	.105	.055	.050	0	↓	540	71.30
65	1.000	.675	.325	.050	0	.035	.240	317	372.20
72	1.190	.660	.530	.060	0	.030	.440	26	337.50
73	.750	.725	.025	0	.025	0	0	2 053	205.00
55	.815	.790	.025	.025	0	↓	↓	1 340	.75
53	.500	.495	.005	.005	↓	↓	↓	107 996	60.00
3	.800	.782	.018	.018	↓	↓	↓	4 179	2.30
4	1.000	.980	.020	.020	↓	↓	↓	1 169	.65
5	1.515	1.245	.270	.270	↓	↓	↓	176	.10

^cSpecimen did not fail.

from the PP failure tests. Additional PP flow tests can be run to increase the data base and reduce the statistical uncertainty in the value of n . Here we will use only data from failure testing because the desired additional flow data are not available. The following correlation is obtained by using the appropriate PP data from table I and is displayed in figure 8:

$$\Delta\epsilon_{el,pp} = 0.0303(\Delta\epsilon_{in})^{0.173} \quad (30)$$

Correlation between cyclic strain-hardening coefficient and hold time.—The elastic strainrange–inelastic strainrange flow relation for cycles involving creep is assumed to be parallel to the corresponding PP line as shown in figure 2. Individual values of K_{ij} are calculated by using equation (6) and the value of n from equation (30). As an example, using the data for specimen 27 from table II gives

$$K_{pc} = (0.0103)(0.00185)^{-0.173} = 0.03059$$

The corresponding hold time is 30 sec. When all of the appropriate values have been determined, the constants A' , α , and m in equation (12) are determined by a multiple linear regression analysis. The results are given here and in figure 9. In a previous publication (ref. 5) the dependency of K_{ij} on total strainrange was ignored.

$$K_{pc} = 0.0480(\Delta\epsilon_t)^{0.087}(t)^{-0.026} \quad (31)$$

$$K_{cp} = 0.0472(\Delta\epsilon_t)^{0.077}(t)^{-0.037} \quad (32)$$

The ability of these equations to correlate the data is shown in figure 10.

Correlation between strain fraction and hold time.—Individual values of F_{ij} are determined from the appropriate data in table II. Using the data for specimen 27 gives

$$F_{pc} = \frac{0.00075}{0.00185} = 0.4054$$

A multiple linear regression analysis leads to the following results:

$$F_{pc} = 0.0088(\Delta\epsilon_t)^{-0.892}(t)^{-0.011} \quad (33)$$

$$F_{cp} = 2.1092(\Delta\epsilon_t)^{0.435}(t)^{0.089} \quad (34)$$

These equations and their ability to correlate the data are shown in figures 11 and 12, respectively.

Correlations to determine mean stress correction.—Correlations of $\Delta\epsilon_{el}$, $\Delta\sigma$, σ_c , and σ_t versus hold time are required to determine the mean stress correction (eqs. (15) and (16)) and are given here. The stresses are in units of megapascals.

Elastic strainrange versus hold time:

$$\Delta\epsilon_{el,pc} = 0.3278(\Delta\epsilon_t)^{0.781}(t)^{-0.008} \quad (35)$$

$$\Delta\epsilon_{el,cp} = 0.2178(\Delta\epsilon_t)^{0.687}(t)^{-0.013} \quad (36)$$

Stress range versus hold time:

$$\Delta\sigma_{pc} = 81\,068(\Delta\epsilon_t)^{0.836}(t)^{-0.004} \quad (37)$$

$$\Delta\sigma_{cp} = 131\,886(\Delta\epsilon_t)^{0.903}(t)^{-0.028} \quad (38)$$

Minimum and maximum stress versus hold time:

$$\sigma_{c,pc} = 216\,313(\Delta\epsilon_t)^{1.179}(t)^{-0.048} \quad (39)$$

$$\sigma_{t,cp} = 192\,882(\Delta\epsilon_t)^{1.142}(t)^{-0.062} \quad (40)$$

These equations and their ability to correlate the data are shown in figures 13 to 18.

The preceding discussion details the steps involved in characterizing the flow behavior of an alloy. A summary of the steps is given here.

(1) The flow relations are sensitive to the way creep is introduced into the cycle. Therefore the flow tests must closely approximate the service cycle to be predicted.

(2) The test specimen is cycled until the criteria for cyclic stability are satisfied.

(3) The minimum stress (σ_c) versus hold time correlation is determined for cycles featuring creep or relaxation in compression (PC cycle), and the maximum stress (σ_t) versus

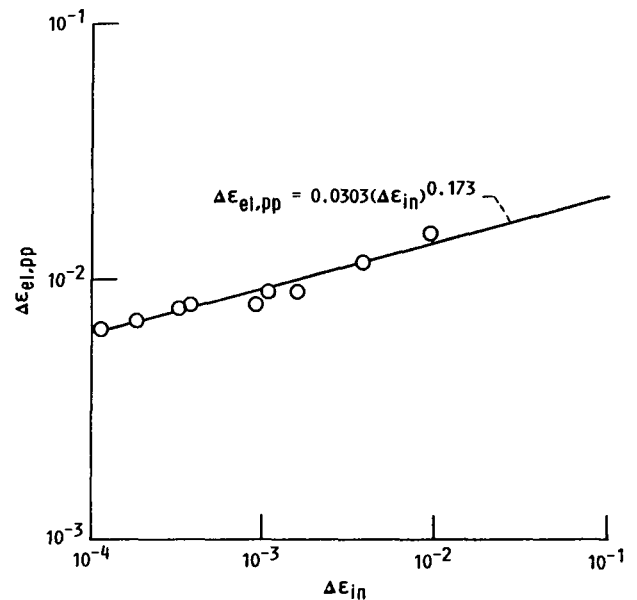


Figure 8.—Relation between elastic and inelastic strainranges for PP cycles: alloy, AF2-1DA; temperature, 760 °C. (Data from ref. 14.)

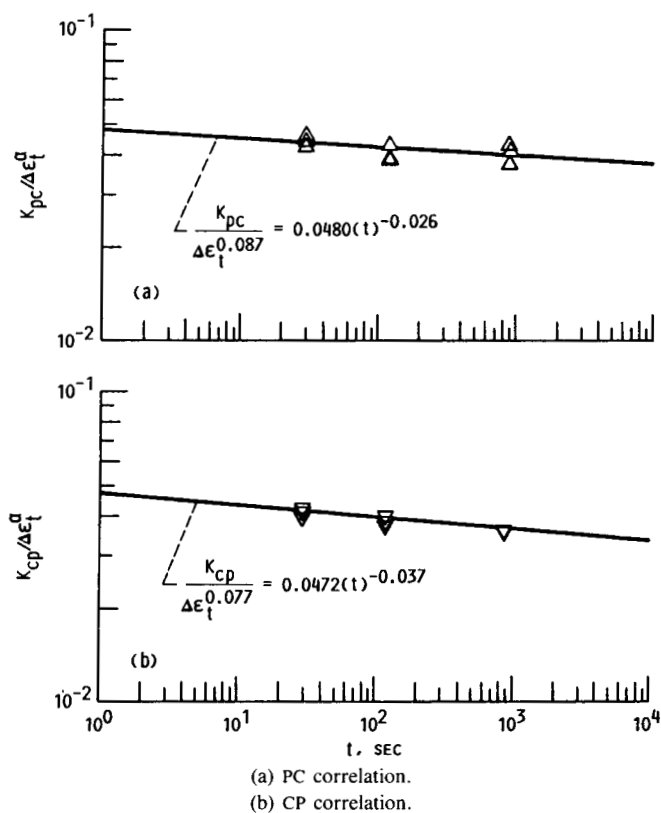


Figure 9.—Relation between cyclic strain-hardening coefficient and hold time for strain-hold cycles: alloy, AF2-1DA; temperature, 760 °C. (Data from ref. 19.)

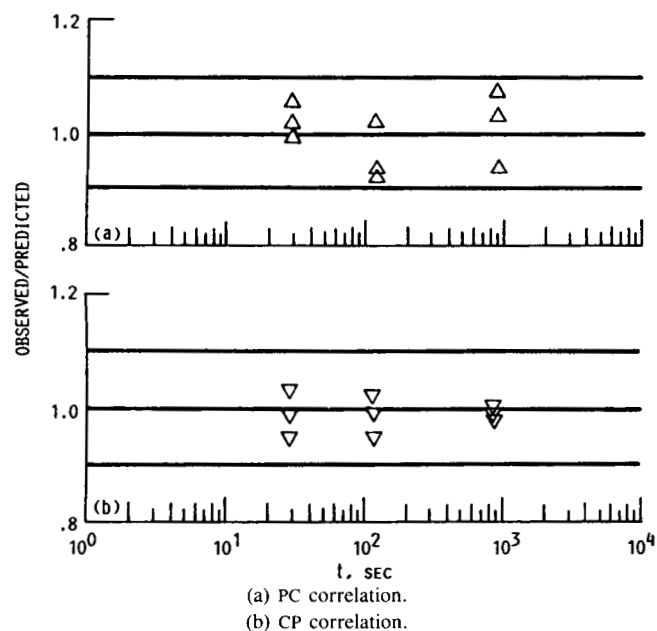


Figure 10.—Ratio of observed to predicted values of cyclic strain-hardening coefficient versus hold time for strain-hold cycles: alloy, AF2-1DA; temperature, 760 °C. (Data from ref. 19.)

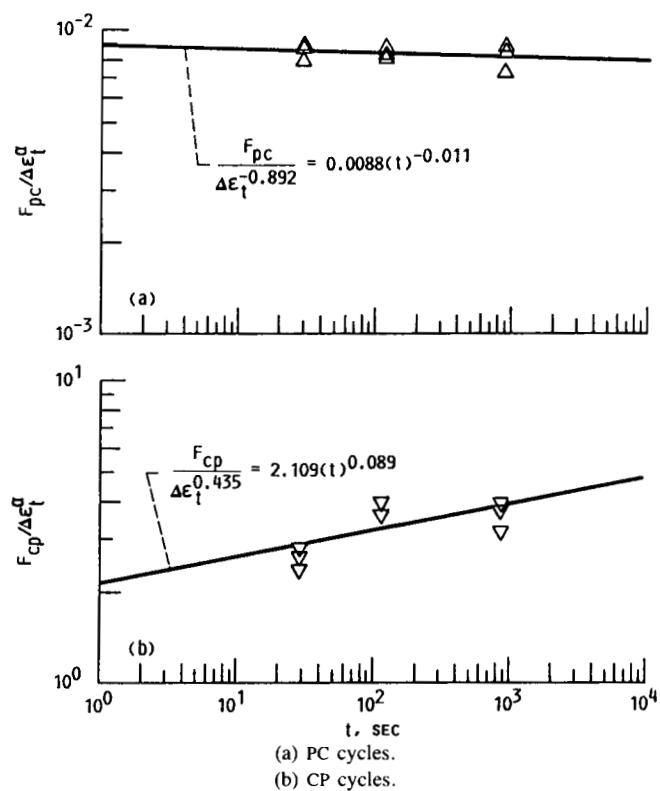


Figure 11.—Relation between strain fraction and hold time for strain-hold cycles: alloy, AF2-1DA; temperature, 760 °C. (Data from ref. 19.)

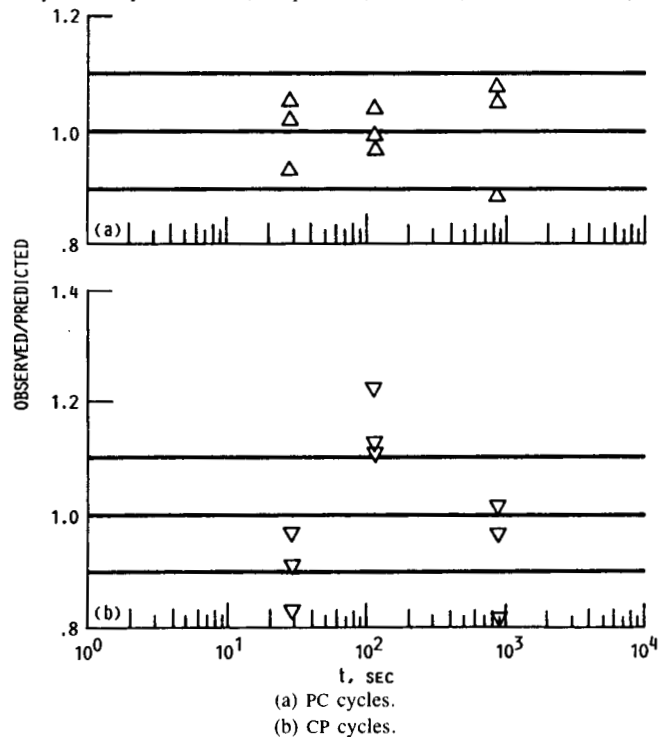


Figure 12.—Ratio of observed to predicted values of strain fraction versus hold time for strain-hold cycles: alloy AF2-1DA; temperature, 760 °C. (Data from ref. 19.)

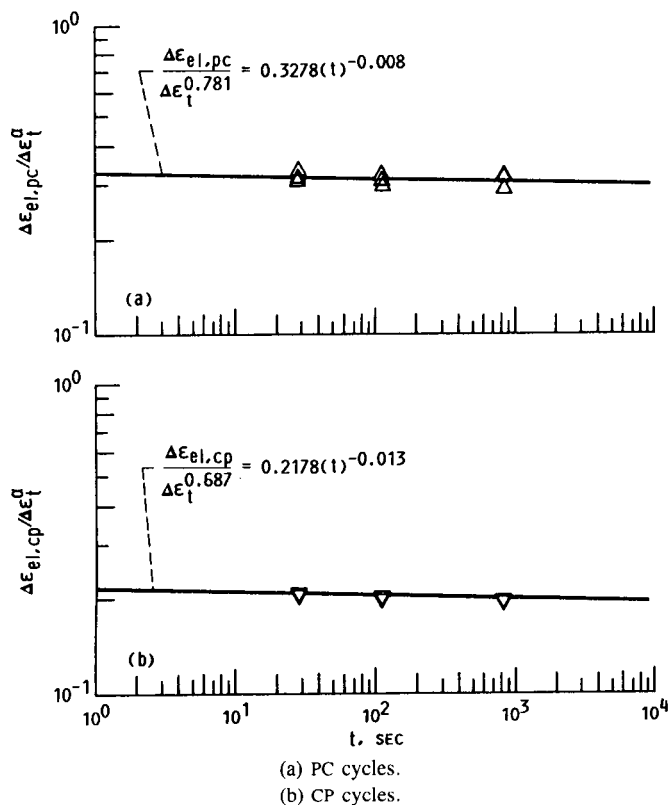


Figure 13.—Relation between elastic strainrange and hold time for strain-hold cycles: alloy, AF2-1DA, temperature, 760 °C. (Data from ref. 19.)

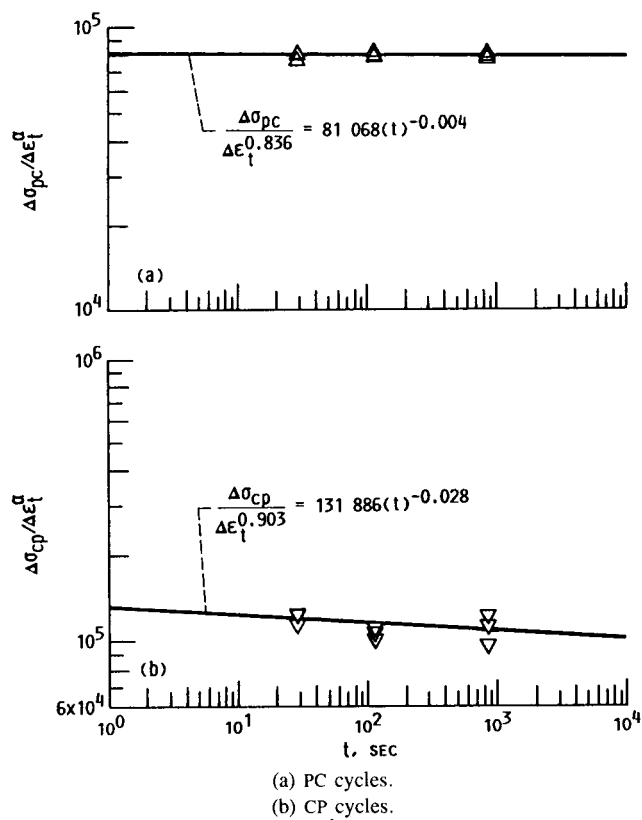


Figure 15.—Relation between stress range and hold time for strain-hold cycles: alloy, AF2-1DA, temperature, 760 °C. (Data from ref. 19.)

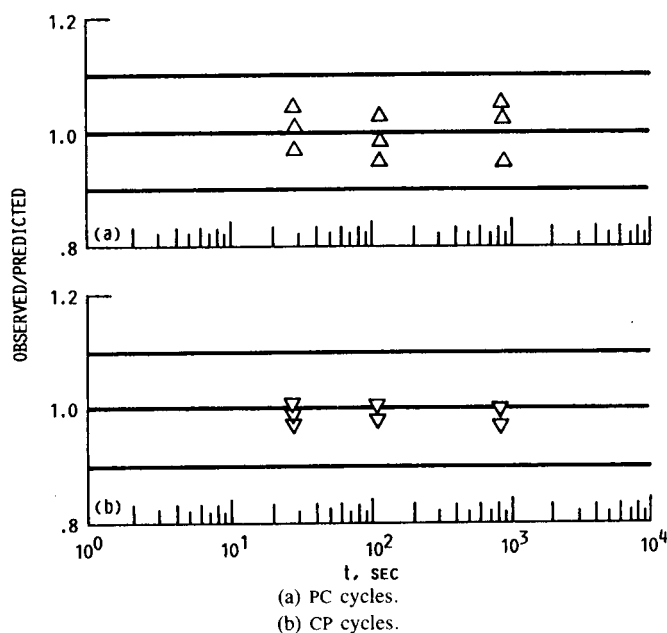


Figure 14.—Ratio of observed to predicted values of elastic strainrange versus hold time for strain-hold cycles: alloy, AF2-1DA, temperature, 760 °C. (Data from ref. 19.)

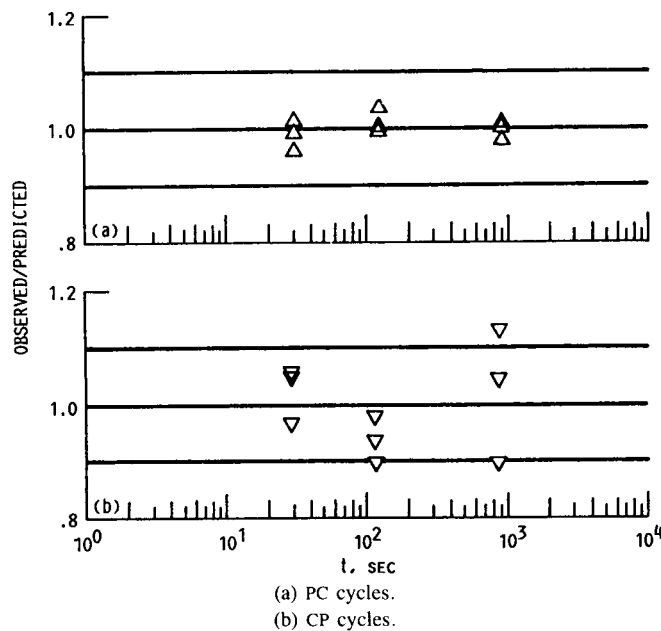


Figure 16.—Ratio of observed to predicted values of stress range versus hold time for strain-hold cycles: alloy, AF2-1DA, temperature, 760 °C. (Data from ref. 19.)

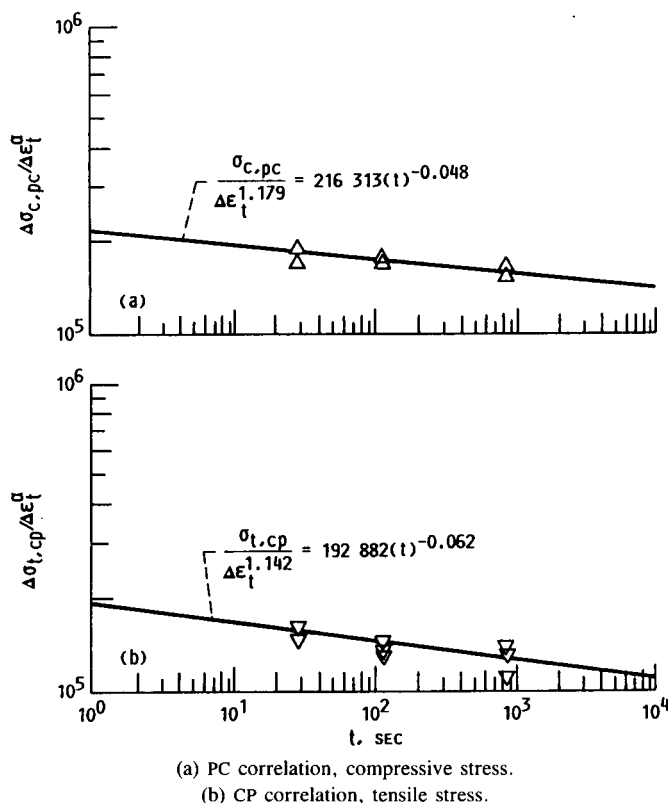


Figure 17.—Relation between stress and hold time for strain-hold cycles: alloy, AF2-1DA; temperature, 760 °C. (Data from ref. 19.)

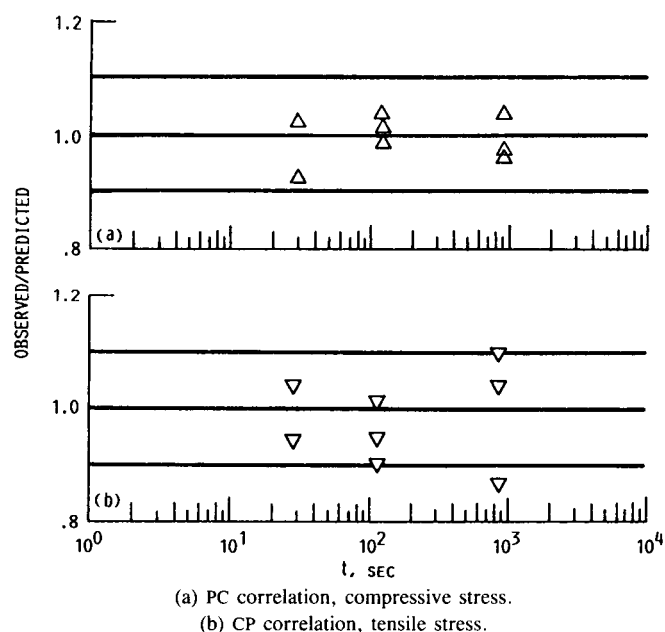


Figure 18.—Ratio of observed to predicted values of stress versus hold time for strain-hold cycles: alloy, AF2-1DA, temperature, 760 °C. (Data from ref. 19.)

hold time correlation is determined for cycles featuring creep or relaxation in tension (CP cycle). These correlations along with the stress range–hold time correlation are used to determine the mean stress present in a cycle of interest.

(4) The procedures described in this section may have to be modified for unusual cycle types. Only conventional stress-hold loads to maximum or minimum strain, strain-hold at maximum or minimum strain, and continuous cycling tests have been utilized to date.

Life Prediction

We now have the information required to predict the lives of PC (CHSC) and CP (THSC) strain-hold cycles. The steps involved are illustrated here by using data for AF2-1DA at 760 °C (ref. 20). The relevant creep-fatigue data are listed in table III. Specimen 243 is used for the example. We must first determine the cycle type, the total strainrange, and the hold time. From table III for specimen 243 the cycle type is PC (CHSC), the total strainrange is 0.0085, and the hold time is 300 sec.

We begin by determining the intercept of the equivalent inelastic line C' in equation (9). From equation (3)

$$C' = [F_{pp}(C_{pp})^{1/c} + F_{pc}(C_{pc})^{1/c}]^c \quad (41)$$

The strain fraction F_{pc} is determined from equation (33).

$$F_{pc} = 0.0088(0.0085)^{-0.892}(300)^{-0.011} = 0.581$$

The values of C_{pp} , C_{pc} , and c are given in figure 7. Solving for C' gives

$$C' = \left[(1-0.581)(0.100)^{1/-0.637} + (0.581)(0.071)^{1/-0.637} \right]^{-0.637} = 0.0802$$

The strain-hardening coefficient K_{pc} is now calculated from equation (31).

$$K_{pc} = 0.0480(0.0085)^{0.087}(300)^{-0.026} = 0.0273$$

Solving for the elastic line intercept B from equation (7) gives

$$B = 0.0273(0.0802)^{0.173} = 0.0176$$

The theoretical zero mean stress life N_{f0} can now be calculated from

$$0.0085 = 0.0176(N_{f0})^{-0.117} + 0.0802(N_{f0})^{-0.637} \quad (42)$$

The value of N_{f0} can be determined by trial and error or directly by using Manson's inversion method (ref. 16). We used the inversion method. Solving for the zero mean stress life gave

$$N_{f0} = 1223 \text{ cycles}$$

TABLE III.—DATA USED FOR LIFE PREDICTION

[Alloy, AF2-1DA; temperature, 760 °C; data from ref. 20.]

(a) Rate data and stresses

Specimen	Test type ^a	Rate data (half-life values)				Stresses (half-life values), MPa					Ratio of mean stress to stress amplitude
		Frequency, Hz	Strain rate in tension and compression, percent/sec	Hold time, sec		Maximum tension	Maximum compression	Maximum range	Relaxation		
				Tension	Compression				Tension	Compression	
239	THSC	0.017	0.67	60.0	0	685.4	912.9	1598.3	109.6	0	-0.142
125	↓	.003	.59	300.0	↓	635.7	902.6	1538.3	112.4	↓	-.174
107		.003	.62	300.0		568.8	900.5	1469.3	93.8		-.226
241		.003	.48	300.0		567.5	863.9	1431.4	73.8		-.207
235	CHSC	.017	.71	0	60.0	932.2	635.7	1567.9	0	93.1	-.189
243	CHSC	.003	.58	0	300.0	904.6	493.7	1398.3	0	46.9	-.294

(b) Strains and failure data

Specimen	Strainranges (half-life values), percent							Cycles to failure, N_f	Time to fail, hr
	Total	EL	IN	PP	PC	CP	CC		
239	1.000	0.820	0.180	0.119	0	0.061	0	771	13.49
125	1.000	.790	.210	.147	↓	.063	↓	1221	101.80
107	.850	.730	.120	.067		.053		1036	86.33
241	.850	.730	.120	.079		.041		1794	149.50
235	1.000	.810	.190	.138		0		433	7.25
243	.850	.760	.090	.064	.026	0	↓	802	66.80

The values required for the mean stress correction are determined by using equations (35), (37), and (39).

$$\Delta\epsilon_{cl} = 0.3278(0.0085)^{0.781}(300)^{-0.008} = 0.0076$$

$$\Delta\sigma_{pc} = 81\,068(0.0085)^{0.836}(300)^{-0.004} = 1472 \text{ MPa}$$

$$\sigma_{c,pc} = 216\,313(0.0085)^{1.179}(300)^{-0.048} = 596 \text{ MPa}$$

The stress amplitude σ_a , the mean stress σ_m , and the stress ratio V_o can now be determined.

$$\sigma_a = \frac{\Delta\sigma}{2} = \frac{1472}{2} = 736 \text{ MPa}$$

$$\sigma_m = 736 - 596 = 140 \text{ MPa}$$

$$V_o = \frac{140}{736} = 0.1902$$

Solving for k from equation (16) and the value of $\Delta\epsilon_{cl}$ calculated previously gives

$$k = \exp \left[-70 \left(\frac{0.0085 - 0.0076}{0.0076} \right)^2 \right] = 0.3747$$

Solving equation (15) for N_{fm} gives

$$N_{fm} = \left[1223^{0.117} - 0.3747(0.1902) \right]^{1/0.117} = 934 \text{ cycles}$$

This compares exceptionally well with the observed life of 802 cycles.

In many situations estimates of the maximum and minimum cyclic lives are of practical interest. In general, maximum life occurs when creep effects are not present in the cycle and life is calculated on a PP basis (fig. 7). Thus equation (9) is written as follows by using equations (13) and (14):

$$0.0085 = 0.022(N_{f0})^{-0.117} + 0.100(N_{f0})^{-0.637} \quad (43)$$

Solving for the zero mean stress life yields

$$N_{f0} = 5147 \text{ cycles}$$

Correcting for mean stress effects by using the k and V_σ values determined previously yields

$$N_{fm} = \left[5147^{0.117} - (0.3747)(0.1902) \right]^{1/0.117} = 4101 \text{ cycles}$$

In general, minimum life occurs if all of the inelastic strain is time dependent (fig. 7). Thus $F_{pp} = 0$ and C' is equal to the intercept of the PC inelastic failure line (eq. (22)). The time-dependent elastic line intercept B is determined from this value of C' , the value of K_{pc} calculated previously, and equation (7).

$$B = 0.0273(0.071)^{0.173} = 0.0173$$

So for minimum life equation (9) is

$$0.0085 = 0.0173(N_{f0})^{-0.117} + 0.071(N_{f0})^{-0.637} \quad (44)$$

Solving for the zero mean stress life gives

$$N_{f0} = 1039 \text{ cycles}$$

Correcting for mean stress effects by using the k and V_σ values calculated previously yields

$$N_{fm} = \left[1039^{0.117} - (0.3747)(0.1902) \right]^{1/0.117} = 789 \text{ cycles}$$

Thus the maximum life of 4101 cycles and the minimum life of 789 cycles bound the observed life of 802 cycles and the predicted life of 934 cycles.

Concluding Remarks

The procedures for characterizing an alloy and predicting cyclic life by using the updated total strain version (TS-SRP) of Strainrange Partitioning have been discussed and examples given. Two aspects of an alloy are characterized: failure behavior, and flow behavior.

Creep-fatigue failure behavior is characterized by conducting tests in the strain regime, where testing times are acceptably short and the inelastic strains are large enough to be measured with good accuracy. Stress-hold tests are the preferred type because of the high creep damage inherent in this type of cycle. Continuous-cycling PP tests are also done to determine the effects of mean stress on cyclic life. Mean stress effects must be known and accounted for when determining the SRP inelastic strainrange versus life relations. These relations are then established for a theoretical zero mean stress condition.

Flow behavior is characterized by cycling the test specimen until the stress-strain hysteresis loop satisfies the criteria for stability. These tests are generally of short duration, and a specimen can be used for more than one test. These tests should be conducted over a spectrum of strainranges and hold times so that an adequate amount of data is available to determine the constants in the flow relations. This serves to reduce uncertainty when predicting life outside the range of the data. Data only from failure tests may be used if necessary, as has been done herein. However, this is not the preferred method.

The analyst now has the information required to predict life in the low-strain regime. The following information is required: total strainrange, hold time, strain rate, and type of cycle (stress hold, strain hold, etc.). The inelastic strainrange versus life relations are not particularly sensitive as to how creep is introduced into the cycle, but the flow relations are. Thus the flow relations must be appropriate for the duty cycle being predicted. The resulting life calculation is for a theoretical zero mean stress condition. This value is then adjusted to account for mean stress.

Lewis Research Center
National Aeronautics and Space Administration
Cleveland, Ohio, Nov. 22, 1988

Appendix—Analysis for Nonparallel Failure Lines

Our experience strongly suggests that assuming that the inelastic and elastic strainrange versus life lines for creep-fatigue cycles are parallel to the corresponding lines for pure fatigue, or PP, cycles is reasonable for isothermal creep-fatigue. And on this basis we have extended this assumption to nonisothermal creep-fatigue. However, this assumption may not be applicable for all alloys, and a method would be required for dealing with such a situation.

If the assumption of parallel lines is not reasonable, then the equations relating failure and flow behavior given here are not applicable. For purposes of discussion let us assume that the inelastic failure lines for creep-fatigue cycles (PC, CP, and CC) are not parallel to the PP line or to each other and that the elastic failure lines for these cycles both translate and rotate as a function of hold time.

Failure behavior is now expressed by the following equations:

$$\Delta\epsilon_{el} = B(N_{f0})^{b'} \quad (45)$$

where $b' = b'(t)$. The four generic SRP life relations are PP cycles:

$$\Delta\epsilon_{in} = C_{pp}(N_{pp})^c \quad (46)$$

and PC, CP, and CC cycles:

$$\Delta\epsilon_{in} = C_{ij}(N_{ij})^{c^*} \quad (47)$$

where c^* is not equal to c and may be different for each type of cycle.

The IDR is written as follows for a creep-fatigue cycle:

$$\frac{F_{pp}}{N_{pp}} + \frac{F_{ij}}{N_{ij}} = \frac{1}{N_{f0}} \quad (48)$$

By using equations (46) and (47) we obtain the following:

$$F_{pp} \left(\frac{C_{pp}}{\Delta\epsilon_{in}} \right)^{1/c} + F_{ij} \left(\frac{C_{ij}}{\Delta\epsilon_{in}} \right)^{1/c^*} = \frac{1}{N_{f0}} \quad (49)$$

Solving for $\Delta\epsilon_{in}$ gives

$$\Delta\epsilon_{in} = C''(N_{f0})^c \quad (50)$$

where

$$C'' = \left[F_{pp}(C_{pp})^{1/c} + F_{ij}(C_{ij})^{1/c^*} (\Delta\epsilon_{in})^{1/c-1/c^*} \right] \quad (51)$$

Flow behavior is expressed by the following equation:

$$\Delta\epsilon_{el} = K_{ij}(\Delta\epsilon_{in})^{n'} \quad (52)$$

Setting equation (45) equal to equation (52) and eliminating N_{f0} by using equation (50) yields

$$B = K_{ij}(C'')^{n'} \quad (53)$$

where $n' = b'/c$.

Since TS-SRP is intended for the low-strain regime, where the elastic strainrange is the dominant term in equation (8), it is reasonable to retain the assumption of parallel inelastic lines and to allow the elastic line to both translate and rotate with hold time. Assuming the inelastic lines to be parallel simplifies the analysis considerably but does not introduce large errors. Thus equation (9) becomes

$$\Delta\epsilon_t = B(N_{f0})^{b'} + C'(N_{f0})^c \quad (54)$$

where $b' = b'(t)$. Since b' is time dependent, it then follows that the strain-hardening exponent n' in equation (52) is also time dependent. The $\Delta\epsilon_{el} - \Delta\epsilon_{in}$ line both translates and rotates with time, and equation (12) cannot be used to determine K_{ij} since this equation accounts only for translation.

The time dependency of the fatigue exponent b' in equation (45) can be determined by conducting flow tests to characterize the time dependency of the strain-hardening exponent n' in equation (52). At this time we are unable to suggest a suitable form for the equations for K_{ij} and n' , but we feel that equation (12) can still be used to correlate the strain fractions F_{ij} and the stress terms $\Delta\sigma$, σ_t , and σ_c .

When the life relations are nonparallel, failure testing will have to include tests at lower strainranges in order to characterize this more complex material behavior.

References

1. Manson, S.S.; Halford, G.R.; and Hirschberg, M.H.: Creep-Fatigue Analysis by Strain-Range Partitioning. Design for Elevated Temperature Environment, ASME, 1971, pp. 12-28.
2. Hirschberg, M.H.; and Halford, G.R.: Use of Strainrange Partitioning to Predict High-Temperature Low-Cycle Fatigue Life. NASA TN D-8072, 1976.
3. Characterization of Low Cycle High Temperature Fatigue by the Strainrange Partitioning Method. AGARD CP-243, AGARD, Paris, France, 1978. (Avail. NTIS, AD-A059900.)
4. Halford, G.R.; and Saltsman, J.F.: Strainrange Partitioning—A Total Strain Range Version. Advances in Life Prediction Methods, D.A. Woodford and J.R. Whitehead, eds., ASME, 1983, pp. 17-26.
5. Saltsman, J.F.; and Halford, G.R.: An Update of the Total-Strain Version of Strainrange Partitioning. Low Cycle Fatigue, ASTM STP-942, H.D. Solomon, G.R. Halford, L.R. Kaisand, and B.N. Leis, eds., American Society for Testing and Materials, Philadelphia, 1987, pp. 329-341.
6. Moreno, V., et al.: Application of Two Creep Fatigue Life Models for the Prediction of Elevated Temperature Crack Initiation of a Nickel Base Alloy. AIAA Paper 85-1420, July 1985.
7. Saltsman, J.F.; and Halford, G.R.: Life Prediction of Thermomechanical Fatigue Using the Total Strain Version of Strainrange Partitioning (SRP): A Proposal. NASA TP-2779, 1988.
8. Halford, G.R., et al.: Bithermal Fatigue—A Link Between Isothermal and Thermomechanical Fatigue. Low Cycle Fatigue, ASTM STP-942, H.D. Solomon, G.R. Halford, L.R. Kaisand, and B.N. Leis, eds., American Society for Testing and Materials, Philadelphia, 1987, pp. 625-637.
9. Halford, G.R.: Low-Cycle Thermal Fatigue. Thermal Stresses II, R.B. Hetnarski, ed., Elsevier, 1987, pp. 330-428.
10. Coffin, L.F., Jr.: The Effect of Frequency on High Temperature, Low Cycle Fatigue. Proceedings of the Air Force Conference on Fracture and Fatigue of Aircraft Structures, H.A. Wood, et al., eds., AFFDL-TR-70-144, 1970, pp. 301-312. (Avail. NTIS, AD-719756.)
11. Halford, G.R.; Saltsman, J.F.; and Kalluri, S.: High Temperature Fatigue Behavior of Haynes 188. Advanced Earth-To-Orbit Propulsion Technology, NASA CP-3012, 1988, pp. 497-509.
12. Manson, S.S.: The Challenge to Unify Treatment of High Temperature Fatigue—A Partisan Proposal Based on Strainrange Partitioning. Fatigue at Elevated Temperatures, ASTM STP-520, A.E. Carden, A.J. McEvily, and C.H. Wells, eds., American Society for Testing and Materials, Philadelphia, 1973, pp. 744-775.
13. Kalluri, S.; Manson, S.S.; and Halford, G.R.: Environmental Degradation of 316 Stainless Steel in High Temperature Low Cycle Fatigue. Proceedings of Third International Conference on Environmental Degradation of Engineering Materials, Penn. State Univ., University Park, PA, 1987, pp. 503-519.
14. Halford, G.R.; and Nachtigall, A.J.: Strainrange Partitioning Behavior of an Advanced Gas Turbine Disk Alloy AF2-1DA. J. Aircr., vol. 17, no. 8, Aug. 1980, pp. 598-604.
15. Halford, G.R.; Saltsman, J.F.; and Hirschberg, M.H.: Ductility-Normalized Strainrange Partitioning Life Relations for Creep-Fatigue Life Predictions. Environmental Degradation of Engineering Materials, M.R. Lothman and R.P. McNitt, eds., Virginia Polytechnic Inst. and State Univ., Blackburg, VA, 1977, pp. 599-612.
16. Manson, S.S.; and Muralidharan, U.: A Single-Expression Formula for Inverting Strain-Life and Stress-Strain Relationships. NASA CR-165347, 1981.
17. Walker, K.P.: Research and Development Program for Nonlinear Structural Modeling With Advanced Time-Temperature Dependent Constitutive Relations. (PWA-5700-50, Pratt & Whitney Aircraft; NASA Contract NAS3-22055.) NASA CR-165533, 1981.
18. Annis, C.G.; Van Wanderham, M.C.; and Wallace, R.M.: Strainrange Partitioning of an Automotive Turbine Alloy. (FR-7424, Pratt & Whitney Aircraft; NASA Contract NAS3-18930.) NASA CR-134974, 1976.
19. Thakker, A.B.; and Cowles, B.A.: Low Strain, Long Life Creep Fatigue of AF2-1DA and INCO 718. (FR-15652, Pratt & Whitney Aircraft; NASA Contract NAS3-22387.) NASA CR-167989, 1983.
20. Hyzak, J.M.: The Effect of Defects on the Fatigue Initiation Process in Two P/M Superalloys. AFWAL-TR-80-4063, 1980. (Avail. NTIS, AD-A093509.)

1. Report No. NASA TM-4102		2. Government Accession No.		3. Recipient's Catalog No.	
4. Title and Subtitle Procedures for Characterizing An Alloy and Predicting Cyclic Life With The Total Strain Version of Strainrange Partitioning				5. Report Date June 1989	
				6. Performing Organization Code	
7. Author(s) James F. Saltsman and Gary R. Halford				8. Performing Organization Report No. E-4457	
				10. Work Unit No. 505-66-11	
9. Performing Organization Name and Address National Aeronautics and Space Administration Lewis Research Center Cleveland, Ohio 44135-3191				11. Contract or Grant No.	
				13. Type of Report and Period Covered Technical Memorandum	
12. Sponsoring Agency Name and Address National Aeronautics and Space Administration Washington, D.C. 20546-0001				14. Sponsoring Agency Code	
15. Supplementary Notes					
16. Abstract The procedures are presented for characterizing an alloy and predicting cyclic life for isothermal and thermo-mechanical fatigue conditions by using the total strain version of Strainrange Partitioning (TS-SRP). Numerical examples are given. Two independent alloy characteristics are deemed important: <i>failure</i> behavior, as reflected by the inelastic strainrange versus cyclic life relations; and <i>flow</i> behavior, as indicated by the cyclic stress-strain-time response (i.e., the constitutive behavior). <i>Failure</i> behavior is characterized by conducting creep-fatigue tests in the strain regime, wherein the testing times are reasonably short and the inelastic strains are large enough to be determined accurately. At large strainranges, stress-hold, strain-limited tests are preferred because a high rate of creep damage per cycle is inherent in this type of test. At small strainranges, strain-hold cycles are more appropriate. <i>Flow</i> behavior is characterized by conducting tests wherein the specimen is usually cycled far short of failure and the wave shape is appropriate for the duty cycle of interest. In characterizing an alloy pure fatigue, or PP, failure tests are conducted first. Then depending on the needs of the analyst a series of creep-fatigue tests are conducted. As many of the three generic SRP cycles are featured as are required to characterize the influence of creep on fatigue life (i.e., CP, PC, and CC cycles, respectively, for tensile creep only, compressive creep only, and both tensile and compressive creep). Any mean stress effects on life also must be determined and accounted for when determining the SRP inelastic strainrange versus life relations for cycles featuring creep. This is particularly true for small strainranges. The life relations thus are established for a theoretical zero mean stress condition.					
17. Key Words (Suggested by Author(s)) Fatigue (Metal); Creep-Fatigue; Life Prediction; Strainrange Partitioning; Constitutive Modeling; Creep; Plasticity; Strain Fatigue				18. Distribution Statement Unclassified - Unlimited Subject Category 39	
19. Security Classif. (of this report) Unclassified		20. Security Classif. (of this page) Unclassified		21. No of pages 24	
				22. Price* A03	